Structural Flexibility of the Linker Region of Human P-Glycoprotein Permits ATP Hydrolysis and Drug Transport†

Christine A. Hrycyna,‡ Lisa E. Airan,‡,§ Ursula A. Germann,‡,|| Suresh V. Ambudkar,‡ Ira Pastan,⊥ and Michael M. Gottesman*,‡

Laboratory of Cell Biology and Laboratory of Molecular Biology, Division of Basic Sciences, National Cancer Institute, National Institutes of Health, Bethesda, Maryland 20892

Received April 20, 1998; Revised Manuscript Received June 23, 1998

ABSTRACT: P-Glycoprotein (Pgp), an energy-dependent drug efflux pump responsible for multidrug resistance of many cancer cells, is comprised of two homologous halves connected by a peptide segment approximately 75 amino acids (aa) in length. The effects of length and composition of this connecting region on Pgp cell surface expression and the ability of the two halves to interact were explored using both stable transfections of Pgp mutants in mammalian cell lines and a vaccinia virus transient expression system. A 17 aa insertion of predicted flexible structure between amino acids 681 and 682 resulted in a functional Pgp molecule that was capable of conferring drug resistance. In contrast, an 18 aa peptide insertion with a predicted α-helical structure was unstable when expressed transiently. A 34 aa deletion from the central core of the linker region (Δ653−686) resulted in a protein expressed at the cell surface in amounts comparable to that of wild-type Pgp but unable to confer drug resistance. No apparent differences in drug or [α-^{32}P]-8-azido-ATP photoaffinity labeling were observed. However, both ATP hydrolysis and drug transport activities of the deletion mutant were completely abrogated, indicating that the linker deletion disconnected substrate binding from ATP hydrolysis and transport. This mutant also failed to exhibit an ATP hydrolysis-dependent enhancement of binding of a conformation-sensitive monoclonal antibody, UIC2. Upon replacement with a 17 aa linker peptide having a predicted flexible secondary structure, but bearing no homology to the deleted 34 aa segment, normal Pgp transport and basal and drug-stimulated ATPase activities were restored along with increased UIC2 binding in the presence of substrate, suggesting a dramatic conformational change between the nonfunctional and functional molecules. Taken together, these data suggest a flexible secondary structure of the connector region is sufficient for the coordinate functioning of the two halves of Pgp, likely specifically required for the proper interaction of the two ATP binding sites.

The successful treatment of metastatic and disseminated cancer depends to a large degree on the effectiveness of cytotoxic anticancer drugs. These chemotherapeutic agents, including the *Vinca* alkaloids, the anthracyclines, the epipodophyllotoxins, Taxol, and actinomycin D, share no common chemistry but are all amphipathic molecules. Unfortunately, most cancers either are intrinsically resistant to treatment with these therapeutic compounds or acquire resistance to a wide spectrum of these agents over time (*1*, *2*). One cause of broad-based cellular resistance is expression of a 170 kDa plasma membrane polypeptide known as the multidrug transporter or P-glycoprotein (Pgp[1]), encoded by the *MDR*1 gene in humans (*3*).

Pgp acts as an energy-dependent pump that reduces the level of accumulation of drugs within cells. ATP binding and hydrolysis are essential for the proper functioning of Pgp (*4*). However, the mechanism by which the energy of ATP hydrolysis is transduced into efficient transport of chemotherapeutic agents out of the plasma membrane or the cytoplasm into the extracellular milieu remains unknown.

Pgp is a 1280 aa polypeptide comprised of two homologous halves. Each half is thought to span the plasma membrane bilayer six times and contains an intracellular ATP binding/utilization domain (*5*). These two halves, which are 43% identical in human Pgp, are connected by a linker peptide of approximately 75 amino acids defined as amino acids 633−709 in human Pgp. This peptide conjoiner, commonly called the linker region, is highly charged (30−40%) and contains the in vivo sites of phosphorylation (*2*). The two halves of Pgp are essential for activity of the transporter as measured by the ability to confer drug resistance or drug-stimulated ATPase activity. These two

† C.A.H. was supported in part by a postdoctoral fellowship from The Jane Coffin Childs Memorial Fund for Medical Research.

* To whom correspondence should be addressed: Laboratory of Cell Biology, Building 37, Room 1A-09, National Cancer Institute, National Institutes of Health, 37 Convent Dr. MSC 4255, Bethesda, MD 20892-4255. Telephone: (301) 496-1530. Fax: (301) 402-0450. E-mail: mgottesman@nih.gov.

‡ Laboratory of Cell Biology.

§ Current address: Washington University, 1 Barnes Jewish Hospital Plaza, Suite 1641 1, St. Louis, MO 63110.

|| Current address: Vertex Pharmaceuticals, Inc., 130 Waverly St., Cambridge, MA 02139-4242.

⊥ Laboratory of Molecular Biology.

[1] Abbreviations: Pgp, P-glycoprotein; aa, amino acid; MDR, multidrug resistance; ABC, ATP-binding cassette; [^{125}I]IAAP, [^{125}I]-iodoarylazidoprazosin; [α-^{32}P]-8-azido-ATP, [α-^{32}P]-8-azidoadenosine 5′-triphosphate; CFTR, cystic fibrosis transmembrane regulator; FACS, fluorescence-activated cell sorting; vanadate, sodium orthovanadate.

S0006-2960(98)00882-4
Published on Web 09/09/1998

domains cannot act autonomously, but appear to act coordinately, suggesting that they interact in some fashion. Mutations made in the Walker A or Walker B consensus sequences in either half of human Pgp reduce or completely abrogate function (*6*) (C. A. Hrycyna, M. R. Ramachandra, I. Pastan, and M. M. Gottesman, unpublished results). Expression of the 725 amino-terminal amino acids of Pgp was not able to render a drug-sensitive mammalian cell multidrug resistant (*7*). Interestingly, drug resistance was not conferred on drug-sensitive NIH3T3 cells upon coexpression of the two halves of Pgp, although stable expression of each half-molecule was detected (*8*). However, upon expression of these molecules in Sf9 insect cells using baculovirus vectors encoding amino acids 1−682 and 683−1280 independently, low-level reconstitution of drug-stimulated ATPase activity was achieved, suggesting that coupling of ATPase activity to transport requires interaction of the two halves (*8*). The low level of reconstituted activity observed with coexpression of each half could be explained by improper orientation of the two halves in vitro, especially considering that no drug resistance was observed upon coexpression of the two halves separately in NIH3T3 cells. However, these experiments did not directly evaluate the role of the linker region in the intact molecule, nor did they address the drug or ATP binding properties of these half-molecules.

Homologous multidrug transporters from mice, rats, hamsters, and yeast have been cloned. Comparison of the primary structures of these proteins revealed remarkable conservation of both the overall predicted topology and sequence. The similarities are most apparent in the ATP binding/utilization domains and most strikingly divergent in the linker region connecting the two halves (*9*). However, since the lengths of these connecting regions are similar, the overall flexibility of the region may be the important consideration for proper folding and interaction of the two halves rather than absolute sequence conservation (*9*, *10*). In fact, in mice, the linker region separating the two halves of the Pgps encoded by mouse *mdr*1a, a multidrug transporter, and *mdr*2, a phosphatidylcholine flippase, can be exchanged with no apparent detrimental effects on function (*11*). Evidence that Pgp has apparently evolved by gene fusion of individually evolved proteins rather than by internal duplication also implies that the linker region may be simply an evolutionary contrivance (*12*). Additionally, the cystic fibrosis transmembrane regulator (CFTR), another member of the superfamily of ATP-dependent transporters to which Pgp belongs, has a much larger 245 aa linker region, known as the R domain, separating its two halves (*13*).

In this study, we sought to determine the functional significance of the region that links the amino- and carboxyl-terminal halves of P-glycoprotein. By insertion and deletion analysis using both stable drug selections and a transient vaccinia virus expression system in mammalian cells, the effects of changing the length and composition of the linker region were evaluated. To enlarge the length of this segment, a 17 aa peptide with a predicted flexible secondary structure was inserted between amino acids 681 and 682 in the linker region. This insertion did not appear to alter the ability of Pgp to confer drug resistance. An 18 aa peptide with predicted α-helical secondary structure was inserted into the same position which resulted in a nonfunctional molecule that was not expressed on the cell surface. To decrease the length of the existing linker region and to study the effects of changing the sequence composition of the linker region, a deletion mutant removing amino acids 653−686 was produced that resulted in a Pgp molecule expressed on the surface but nonfunctional in transport or drug-stimulated ATPase assays. Upon insertion of a 17 aa flexible peptide into this deletion mutant, the ability to confer drug resistance, basal and drug-stimulated ATPase activity, in vitro transport function, and interaction with the conformation-sensitive monoclonal antibody UIC2 was restored to at least 80% of wild-type Pgp levels. Taken together, these data suggest that a flexible connector region is sufficient for coordinating the function of these two domains, most likely specifically involving the two ATP sites.

EXPERIMENTAL PROCEDURES

Materials. Minimum essential medium with Earle's salts (EMEM), Opti-Eagle's minimal essential medium (OPTI-MEM), Iscove's modified Dulbecco's medium (IMDM), fetal bovine serum (FBS), calf serum, Dulbecco's modified Eagle's medium (DMEM) without glucose and phenol red, trypsin, and Lipofectin were obtained from Life Technologies, Inc. (Grand Island, NY). DMEM was from Quality Biological (Gaithersburg, MD). [^{125}I]Iodoarylazidoprazosin ([^{125}I]IAAP) was from NEN DuPont (Boston, MA). 4-(2-Aminoethyl)benzenesulfonyl fluoride hydrochloride (AEBSF) was from ICN (Irvine, CA). Cyclosporin A was from Calbiochem (San Diego, CA), and rhodamine 123 was from Kodak Co. (New Haven, CT). Calcein-AM was from Molecular Probes (Eugene, OR). Geneticin (G418-sulfate) was obtained from Life Technologies, Inc. pSV2-neo was obtained from Clontech (Palo Alto, CA). All other chemicals were obtained from Sigma (St. Louis, MO). Enzymes used for recombinant DNA techniques were from New England Biolabs (Beverly, MA).

Cell Lines and Viruses. Human osteosarcoma (HOS) (ATCC catalog no. CRL1543) cells were propagated as monolayer cultures at 37 °C in 5% CO_2 in EMEM supplemented with 4.5 g/L glucose, 5 mM L-glutamine, 50 units/mL penicillin, 50 μg/mL streptomycin, and 10% FBS. Human HeLa and murine NIH3T3 cells were grown as monolayer cultures in DMEM supplemented with 4.5 g/L glucose, 5 mM L-glutamine, 50 units/mL penicillin, 50 μg/mL streptomycin, and 10% FBS or 10% calf serum. Recombinant vaccinia virus encoding bacteriophage T7 RNA polymerase (vTF7-3), required for the expression of the gene controlled by the T7 promoter in a transfected plasmid, was obtained from B. Moss (National Institutes of Health, Bethesda, MD). vTF7-3 was propagated and purified as previously described (*14*, *15*).

Antibodies. The human-specific monoclonal antibody MRK-16 was a gift from Hoechst Japan Ltd. (*16*). The polyclonal antibodies PEPG12 and PEPG13 were developed in this laboratory (*17*). The human-specific monoclonal antibody UIC2 was from Immunotech (Westbrook, ME). Purified mouse IgG2a and FITC-labeled anti-mouse IgG2a secondary antibody were purchased from PharMingen (San Diego, CA). Goat anti-rabbit IgG conjugated with peroxidase was from Life Technologies, Inc.

Retroviral Expression Vector Constructs. (A) Insertion Mutants. Fifty-one- and 54-base pair sequences and their

complements were synthesized (Applied Biosystems) for insertion into the unique *Hin*dIII site at nucleotide position 2042 within the connecting region of P-glycoprotein: flexible insertion peptide oligonucleotide (coding strand), 5′-AGCTTGGAGGCGGTGGCTCGGGCGGTGGCGGCTCGGGTGGCGGCGGCTCTA-3′; and α-helical peptide insertion oligonucleotide (coding strand), 5′-AGCTTGCTGAAGCGGCCGCAAAGGAAGCTGCAGCCAAGGAGGCTGCAAAGGCCA-3′.

The inserts were synthesized such that they would anneal into a *Hin*dIII-digested vector and reconstitute two *Hin*dIII restriction sites on either side of the insert. Newly synthesized oligonucleotides were purified, and the trityl group was removed on an oligonucleotide purification column (Applied Biosystems). Complementary oligonucleotides were then annealed and ligated into the unique *Hin*dIII site of the *MDR*1 cDNA in the cloning vector pSX-*MDR*1/A. pSX-*MDR*1/A is a pGEM3-based vector in which the multiple cloning site has been eliminated and replaced with a *Sac*II−*Xho*I site to introduce a cDNA encoding the G185V *MDR*1 variant. pSX-*MDR*1/A subclones containing the human *MDR*1 gene and insert sequences were identified by digestion with *Hin*dIII and subsequent polyacrylamide gel (5%) electrophoresis. To verify the sequence and to identify clones containing the insert in the correct orientation, DNA sequence analysis over the flanking regions and the entire insert was performed (*18*). Subsequently, the modified genes were excised from pSX-*MDR*1/A with *Sac*II and *Xho*l and ligated into retroviral expression vectors, i.e., pHa*MDR*1/A (for the α-helical experiments) (*19*) and pSK4ADA (for the flexible linker experiments) (*20*).

(B) Deletion Mutant. pSX-*MDR*1/A-(Δ653−686) was constructed by replacing the *Cla*I−*Xba*I fragment in pSX-*MDR*1A-WT-CX (*21*) with annealed oligonucleotides UAG112 (5′-CGATGCCTTGGAAGCT-3′) and UAG113 (5′-CTAGAGCTTCCAAGGCAT-3′). After confirmation of the nucleotide sequence, the cDNA encoding the *MDR*1-(Δ653−686) deletion mutant was transferred as a *Sac*II−*Xho*I fragment into a retroviral expression vector (*19*) to yield pHa*MDR*1/A-(Δ653−686).

(C) Replacement Mutant. pHa-*MDR*1-(17 aa replacement) was constructed by swapping the *Nsi*I−*Xho*I fragment from pTM1-*MDR*1-(17 aa replacement) (see below) into pHa-*MDR*1-(wild-type) carrying the wild-type gene (*22*).

Vaccinia Virus Expression Vector Construction. To construct pTM1-*MDR*1-(Δ653−686), the *Xba*I and *Cla*I restriction sites and the 598-base pair segment between them were removed from the original expression vector pTM1-*MDR*1-(wild-type)·His_6 (*23*) by digestion, Klenow treatment, and blunt-end ligation using standard techniques (*24*). These sites were located in a nonessential part of the original plasmid, and their removal did not affect expression of Pgp. This plasmid, termed pTM1(ΔX/ΔC)-*MDR*1, was subsequently cut with *Eco*RI and *Nde*I and replaced with the same fragment from pHa-*MDR*1/A-(Δ653−686). The resultant plasmid was termed pTM1-*MDR*1-(Δ653−686) and contains *Cla*I and *Xba*I restriction sites flanking the 34 aa deletion. These plasmids have a six-histidine tag at the C terminus of the protein which did not alter expression or activity of the transporter (*25*).

To synthesize the 17 aa flexible replacement linker, complementary 78-base pair sequences were synthesized commercially (Life Technologies, Gaithersburg, MD). Flanking the insertion sequence, these oligonucleotides contained the sequence for the *Cla*I and *Xba*I restriction sites: coding strand sequence, 5′-CC ATC GAT GCC TTG GAA GGT GGT GGT GGT AGT GGT GGT GGT GGT AGT GGT GGT GGT GGT AGT GGT AGT GCT CTA GAG C-3′. These oligonucleotides were annealed using standard techniques (*24*), cut with *Xba*I and *Cla*I, purified, and annealed to the similarly digested parent vector, pTM1-*MDR*1-(Δ653−686), to produce pTM1-*MDR*1-(17 aa replacement). To create the pTM1-*MDR*1-(α-helix insertion), the *Nsi*I−*Xho*I fragment was swapped between pHa-*MDR*1-(α-helix insertion) and pTM1-*MDR*1. The sequences in the constructs were verified by automated sequencing using the PRISM Ready Reaction DyeDeoxy Terminator Sequencing Kit (Perkin-Elmer Corp., Norwalk, CT).

Cell Transfections and Drug Selection. Drug-sensitive NIH3T3 cells were transfected with variants of the wild-type pHa*MDR*1/A (G185) retroviral vector (*22*, *26*) by the calcium phosphate coprecipitation method (*27*). Ten micrograms of plasmid DNA was used to transfect 3.5×10^5 cells/25 cm^2 tissue culture flask that were fed with fresh DMEM 3 h before transfection. Eighteen hours after transfection, the cells were washed once and fed with complete DMEM. After an additional 24 h, the cells were split 1:3 into 100 mm dishes in complete DMEM containing 30 or 50 ng/mL vincristine. The cells were then incubated for 12 days at 37 °C in 5% CO_2. Colonies from one dish were stained with 0.5% (w:v) methylene blue in 50% (v:v) ethanol and counted manually. Transfectant colonies from the remaining dishes were expanded and maintained in their respective medium containing 30 or 50 ng/mL vincristine and subsequently subjected to FACS analysis.

Transfections followed by colchicine selection with the modified pSK4ADA-*MDR*1 (G185V) DNA (flexible linker experiments) and modified pHa*MDR*1/A (G185V) DNA (α-helical experiments) were performed similarly but using 100 mm dishes throughout. Eighteen hours after transfection, cells were washed three times and fed with DMEM supplemented with 5% calf serum. Twenty-four hours later, the cells were split 1:4 into selective media containing colchicine at a concentration of 60 ng/mL. After 12 days, colonies were counted manually after staining with 0.5% (w:v) methylene blue in 50% (v:v) ethanol.

Expression of Pgp by a Recombinant Vaccinia Virus-Mediated Infection−Transfection Protocol. A 70−80% confluent monolayer of HOS or HeLa cells grown in 75 cm^2 tissue culture flasks was infected with vTF7-3 and transfected with pTM1-*MDR*1 constructs as described previously (*23*). HOS cells were fed with 12 mL of EMEM supplemented with 10% FBS, and HeLa cells were fed with 12 mL of DMEM supplemented with 10% FBS after 4 h and incubated for the indicated periods of time at 32 °C in the presence of 5% CO_2.

Preparation of Crude Membranes. Cells were harvested by scraping and washed twice in ice-cold phosphate-buffered saline (PBS) containing 1% aprotinin (Sigma, catalog no. A6279). All subsequent procedures were carried out at 4 °C. The cell pellet was resuspended in hypotonic lysis buffer [10 mM Tris (pH 7.5), 10 mM NaCl, 1 mM $MgCl_2$, 1 mM DTT, 1 mM AEBSF, and 1% aprotinin (Sigma, catalog no. A6279)] in a volume of approximately 0.5 mL/75 cm^2 tissue

culture flask and frozen at −80 °C. Subsequently, the cells were thawed and incubated on ice for 30−45 min and disrupted using 50 strokes with a Dounce homogenizer using tight fitting pestle A only. The homogenate was diluted 2-fold with hypotonic lysis buffer and subsequently spun at 500*g* for 10 min to remove the undisrupted cells and nuclear debris. The low-speed supernatant was transferred to a new tube and incubated with micrococcal nuclease (50 units/mL) in the presence of 1 mM $CaCl_2$ for 20−30 min on ice. The membranes were collected by centrifugation for 30 min at 300000*g* and resuspended in 300−500 μL of resuspension buffer containing 10% glycerol using a 1 mL syringe and a blunt-ended 23 gauge needle. The resuspended membranes were stored in 50 μL aliquots at −70 °C immediately, and the protein content was determined by a modified Lowry method using bovine serum albumin as a standard (*28*).

SDS−Polyacrylamide Gel Electrophoresis (SDS−PAGE) and Immunoblot Analysis. SDS−PAGE and immunoblot analysis were performed as described (*23*) except that samples were incubated in Laemmli SDS−PAGE sample loading buffer (*29*) at room temperature for 30 min. PEPG13 was used at a 1:4000 dilution in 5% (w:v) nonfat dry milk dissolved in PBS containing 0.05% (v:v) Tween 20 (PBST). The secondary antibody solution was a 1:10000 dilution of goat anti-rabbit IgG conjugated with peroxidase in 5% (w:v) nonfat dry milk dissolved in PBST.

[α-^{32}P]-8-Azidoadenosine 5′-Triphosphate ([α-^{32}P]-8-Azido-ATP) Labeling of Pgp and Immunoprecipitation. Membrane protein (50 μg of total protein) was diluted in labeling buffer containing 50 mM Tris-HCl (pH 7.5), 1% (v:v) aprotinin solution (Sigma, catalog no. A6279), 1 mM AEBSF (ICN, Irvine, CA), and 10 mM $MgCl_2$ (final concentration) to a final volume of 97.5 μL in a 1.5 mL microcentrifuge tube. The samples were incubated on ice for 3 min; 5 μCi of [α-^{32}P]-8-azido-ATP (∼2.5 μM final concentration) (specific activity of 23 Ci/mmol, 2.0 mCi/mL) (ICN, catalog no. 37015) was added per tube under subdued light conditions, and the mixtures were incubated in the dark for 10 min on ice. For vanadate trapping experiments, samples were preincubated in the presence of 300 μM vanadate for 3 min at room temperature, and after addition of 5 μCi of [α-^{32}P]-8-azido-ATP, the samples were further incubated at 37 °C for 10 min under subdued light conditions. Samples were then exposed to a UV lamp at 365 nm (Black-Ray lamp, model XX-15 from UVP, Upland, CA) for 15 min on ice to facilitate cross-linking. The cross-linked products were then subjected to immunoprecipitation. Six hundred microliters of 1× cold RIPA buffer [20 mM Tris-HCl (pH 7.2), 150 mM NaCl, 1% (v:v) Triton X-100, 1% (w:v) sodium deoxycholate, 0.1% (w:v) sodium dodecyl sulfate, and 1 mM ethylenediaminetetraacetic acid (EDTA)] containing a 1% (v:v) aprotinin solution (Sigma, catalog no. A6279) and 1 mM AEBSF and 8 μL of PEPG13 or PEPG12 polyclonal antibody was added to each sample. The tubes were then incubated at 4 °C for 1 h on a rotary shaker. Twenty-five microliters of Protein A Agarose beads [45−55% suspension in 20 mM sodium phosphate (pH 7.2), 0.15 M NaCl, and 0.02% (w/v) merthiolate (Life Technologies, Grand Island, NY, catalog no. 15918-014)] was added to each sample, and the incubation was allowed to continue at 4 °C for an additional 2−3 h. The samples were centrifuged at 14000*g* for 10 s, and the supernatant was removed by gentle aspiration. The beads were then washed three times with 1 mL of 1× cold RIPA buffer. The bound protein was eluted by incubation with 30 μL of 2× SDS−PAGE sample buffer at room temperature for 30−60 min. The samples, including the beads, were subjected to SDS−PAGE. The gel was subsequently fixed in a solution containing 30% (v:v) methanol and 10% (v:v) acetic acid for 30 min, dried, and subjected to autoradiography.

Drug Photoaffinity Labeling. Photoaffinity labeling of Pgp with [^{125}I]IAAP (specific activity, 2200 Ci/mmol) was performed with intact cells as previously described (*23*, *30*) with minor modifications. After photo-cross-linking, cells (1×10^6 cells/100 μL of lysis buffer) were lysed by three freeze−thaw cycles in lysis buffer containing 10 mM Tris (pH 8.0), 0.1% (v:v) Triton X-100, 10 mM $MgSO_4$, 2 mM $CaCl_2$, and 1 mM ditihiothreitol (DTT). AEBSF (2 mM), 1% (v:v) aprotinin solution (Sigma, catalog no. A6279), and 50 units/mL micrococcal nuclease (*Staphylococcus aureus*) (Pharmacia Biotech, Piscataway, NJ, catalog no. 27-0584-01) in the presence of 1 mM $CaCl_2$ were added to the lysis buffer just prior to use. The lysates were subjected to SDS−PAGE with subsequent autoradiography.

Measurement of ATPase Activity. Pgp-associated ATPase activity was measured by determining the level of sodium orthovanadate-sensitive release of inorganic phosphate from ATP with a colorimetric method as described (*23*, *31*) with some further modifications. Membrane suspensions (20 μg) were first incubated at 37 °C for 5 min in a reaction mixture containing 50 mM Tris-HCl (pH 7.5), 5 mM sodium azide, 2 mM [ethylenebis(oxyethylenenitrilo)]tetraacetic acid (EGTA, pH 7.0), 2 mM ouabain, 2 mM dithiothreitol (DTT), 50 mM KCl, and 10 mM $MgCl_2$. The drugs were added from stock solutions prepared in dimethyl sulfoxide, and the assay mixtures were then incubated for 3 min at 37 °C. The final concentration of dimethyl sulfoxide in the assay medium was 1%, a concentration that does not exhibit any effect on the ATPase activity. The reactions were then started by the addition of 5 mM ATP to the assay mixtures (a total volume of 100 μL) and the mixtures incubated at 37 °C for 20 min. Reactions were stopped by the addition of 100 μL of 5% SDS solution, and the amount of inorganic phosphate released was measured by a colorimetric reaction (*31*). This reaction involves the formation of a colored complex in the presence of 1% ammonium molybdate in 2.5 N sulfuric acid, 0.014% antimony potassium tartarate, and 1% (w:v) ascorbic acid. Following a 10 min incubation at room temperature, the optical density at 880 nm is read and used to quantitate the amount of phosphate released ($1\ OD_{880} = \sim 58-62$ nmol of inorganic phosphate). The vanadate-sensitive activities were calculated as the differences between the ATPase activities obtained in the absence and presence of 300 μM vanadate.

Fluorescence-Activated Cell Sorting (FACS) Analysis. FACS analysis was carried out using a FACSort flow cytometer equipped with CellQuest software (Beckton-Dickinson FACS system, San Jose, CA).

Determination of Cell Surface Expression of Pgp by MRK-16 Staining and FACS Analysis. Cells were removed from flasks 24 h after infection-transfection by trypsinization, washed, and resuspended in IMDM supplemented with 5% FBS. To determine cell surface expression, 500 000 cells were incubated with 6 μg of MRK-16 or purified mouse

IgG2a (as a control) in 200 μL of the same medium and the mixtures incubated at 4 °C for 30 min. Cell suspensions were then diluted to 5 mL in cold medium and centrifuged at 200*g* for 5 min. Washed cell pellets were resuspended in 200 μL of cold IMDM containing 2 μg of FITC-labeled anti-mouse IgG and incubated at 4 °C for 30−45 min. Cells were washed as above and resuspended in 350 μL of cold PBS and analyzed by FACS.

UIC2 Reactivity Shift Assays. Cells were harvested and washed as described above for MRK-16 staining. The cells (500 000) were preincubated for 3 min at 37 °C and for an additional 5 min with or without 5 μM cyclosporin A (final concentration) in a final volume of 400 μL. Subsequently, 5 μg of UIC2 was added to the cell suspensions, and the mixtures were incubated at 37 °C for 30 min. The cell suspensions were then diluted to 5 mL in IMDM supplemented with 5% FBS and centrifuged at 200*g* for 5 min. Washed cell pellets were resuspended in 400 μL of medium containing 1 μg of FITC-labeled anti-mouse IgG and incubated at 37 °C for 30 min. Cells were washed as above and resuspended in 400 μL of cold PBS and analyzed by FACS.

Fluorescent Drug Accumulation Assays. Cells were harvested and washed as described above for MRK-16 staining. Subsequently, 500 000 cells were incubated in 5 mL of IMDM (prewarmed to 37 °C) containing 5% FBS and the fluorescent drug substrate with or without 5−7.5 μM cyclosporin A for 40 min at 37 °C in 6 mL polystyrene tubes. Rhodamine 123 was used at a final concentration of 0.5 μg/mL. The cells were then centrifuged at 200*g* for 5 min; the medium was removed by aspiration, and the cell pellet was resuspended in 350 μL of ice-cold PBS and analyzed by FACS. For rhodamine 123 measurements, the cells were resuspended in 4.5 mL of substrate-free medium with or without 5−7.5 μM cyclosporin A and incubated for an additional 40 min at 37 °C. The cells were pelleted by centrifugation at 200*g* for 5 min, and the medium was removed by aspiration. The cells were then resuspended in 350 μL of ice-cold PBS and analyzed by FACS.

RESULTS

Insertion of a Flexible Peptide into the Linker Region of Pgp Does Not Significantly Affect Function. The general strategy employed in these studies was to place sequences of amino acids with either a predicted flexible or α-helical secondary structure into the linker region of the multidrug resistance protein, Pgp, between amino acids 681 and 682 to determine if these insertions would affect its function. As defined in Figure 1A, the connecting region is a short stretch of approximately 75 nonconserved amino acids that separates the amino- and carboxyl-terminal halves of the protein. A 17 aa sequence previously determined to be flexible in its secondary structure (*32*) was chosen as a candidate for insertion into the connecting region of Pgp. The cDNA insert was synthesized as described in Experimental Procedures and was cloned into the unique *Hin*dIII site between the coding sequence for amino acids K681 and L682 (Figure 1B). The *MDR*1 construct containing the insert in the correct orientation was cloned into the retroviral expression vector pSK4ADA, transfected into the murine NIH3T3 cell line, and selected in 60 ng/mL colchicine. Table 1 demonstrates that similar numbers of drug-resistant colonies were obtained with unmodified *MDR*1 and *MDR*1-(flexible insertion), indicating that the modified transporter was approximately as effective as the G185V variant Pgp in conferring resistance to colchicine. These resultant drug-resistant cells expressed modified human Pgp on their cell surface, as demonstrated by immunofluorescence using the human-specific monoclonal anti-Pgp antibody MRK-16 (data not shown). These data suggest that this 17 aa flexible insertion minimally altered the functional properties of Pgp. The experiments described in Table 1 were performed with the G185V variant of Pgp, a well-characterized mutant that has been shown to change the substrate specificity of Pgp compared to that of the wild type, increasing its ability to confer resistance to colchicine (*23*). We found that the insertion mutant in Table 1 does not have an altered phenotype compared to the G185V variant, suggesting that the insertion of these additional amino acid residues did not affect the ability of the transporter to confer resistance to colchicine.

Insertion of an α-Helical Peptide into the Linker Region of Pgp Affects the Cell Surface Localization of Pgp. Subsequently, a sequence with a similar length but having a predicted α-helical secondary structure was inserted into the same site in the Pgp linker region to determine if the addition of more defined structure would be deleterious. It has been previously determined that short alanine-based peptides form stable α-helices in H_2O when separated by glutamic acid-lysine pairs (*33*, *34*). To this end, a complementary pair of 54-base pair oligonucleotides was synthesized and annealed into the unique *Hin*dIII site between the coding sequence for amino acids 681 and 682 in Pgp. This insertion sequence is an 18 aa alanine-based peptide predicted to have α-helical secondary structure (α-helix insertion) (Figure 1B).

This modified *MDR*1 cDNA was cloned into pHa*MDR*1/A, transfected into the murine NIH3T3 cell line, and selected with 60 ng/mL colchicine. As seen in Table 1, transfection with pHa*MDR*1-(α-helix insertion), containing the sequence for the α-helical peptide insertion, yielded no colchicine-resistant cells. To further examine the failure of the α-helical peptide insertion to confer drug resistance, parental G185V Pgp and the α-helical peptide insertion construct were transfected into NIH3T3 cells and the resultant transiently expressing populations were analyzed by FACS. The cells transfected with the α-helical insertion construct were found to express little or no Pgp at the plasma membrane compared to those expressing pHa*MDR*1/A (data not shown). Stable transfectants generated with a pHa*MDR*1(α-helix insertion)-IRES-TK (thymidine kinase)-type construct (*35*) yielded HAT-selected Ltk^- colonies that were MRK-16-negative (data not shown).

The Pgp construct containing the α-helical peptide insertion was subsequently cloned into the pTM1-*MDR*1 vector and transiently expressed in HeLa cells infected with the vaccinia virus vTF7-3 (*23*). This expression system is ideal for the study of nonfunctional as well as functional constructs because high levels of protein are made without imposing drug selection (*36*). As shown in Figure 2, wild-type Pgp was expressed at high levels in approximately 80% of the cells. However, Pgp-(α-helix insertion) was not expressed at the cell surface compared to wild-type Pgp and was virtually indistinguishable from the vector only (pTM1) control. The addition of cyclosporin A has previously been

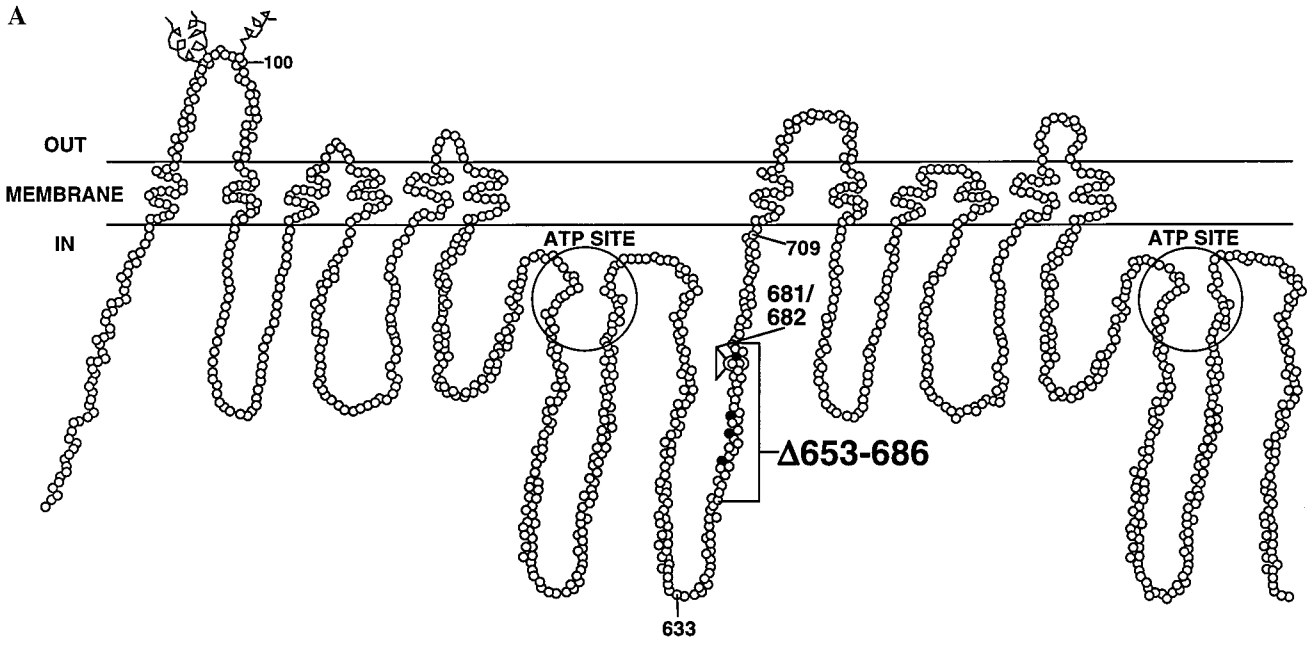

B

Pgp-(flexible insertion):

aa 681 682

K L G G G G S G G G G S G G G G S K L

AAG CTT GGA GGC GGT GGC TCG GGC GGT GGC GGC TCG GGT GGC GGC GGC TCT AAG CTT

Pgp-(α-helix insertion):

aa 681 682

K L A E A A A K E A A A K E A A K A K L

AAG CTT GCT GAA GCG GCC GCA AAG GAA GCT GCA GCC AAG GAG GCT GCA AAG GCC AAG CTT

Pgp-(17aa replacement):

aa 652 687

E G G G V S G G G G S G G G G S G S A

GAA GGT GGT GGT GTT AGT GGT GGT GGT GGT AGT GGT GGT GGT GGT AGT GGT AGT GCT

FIGURE 1: (A) Two-dimensional hypothetical model of Pgp structure based on hydropathy plot analysis of the primary amino acid sequence. The ATP binding/utilization domains are circled. Putative glycosylation sites in the first extracellular loop are represented by squiggly lines. The region including amino acids 633−709 is defined as the linker or connector region. This region contains the known phosphorylated serine residues at positions 661, 667, 671, and 683 shown as darkened circles. Peptide insertion sequences were placed between amino acids 681 and 682. The partial linker region deletion mutant, Pgp-(Δ653−686), is demarcated by a bracket (adapted from refs *1* and *2*). (B) Nucleotide and amino acid sequences of linker region insertion and replacement peptides. The 17 aa replacement is also predicted to have a flexible secondary structure.

Table 1: Summary of Transfections of NIH3T3 Cells with *MDR*1 Constructs Containing Sequences Encoding Flexible and α-Helical Peptide Insertions in the Linker Region of Pgp[a]

DNA	expt 1[b]	expt 2	expt 3	expt 4
pSK4ADA-*MDR*1 (unmodified)	134	26	59	74
pSK4ADA-*MDR*1 (flexible insertion)	174	32	56	61
pHaMDR1/A (unmodified)	36	54	62	63
pHaMDR1/A (α-helix insertion)	0	0	0	0

[a] Cells were selected and maintained in 60 ng/mL colchicine because the *MDR*1 gene that was used contains a Gly → Val mutation at position 185. [b] Values are expressed as the number of colonies per microgram of DNA. In each experiment, 100 mm dishes were stained and the colonies counted as described in Experimental Procedures. Averages from each experiment are shown. Controls without DNA yielded zero to two colonies per dish and have been subtracted.

shown to facilitate the cell surface expression of some mutant Pgp molecules (*37*). Expression of Pgp-(α-helix insertion) under similar conditions in the presence of 10 μM cyclosporin A resulted in only a slight, and most likely insignificant, increase in the amount of protein present at the cell surface (Figure 2). Immunoblot analysis using polyclonal antibody PEPG13 demonstrated that virtually no full-length Pgp, migrating at a molecular mass of approximately 140 kDa, containing the α-helical peptide insertion was being expressed in these cells (Figure 3). This construct appeared to be expressed at levels comparable to that of the wild-type protein but was being degraded. Not surprisingly, membrane preparations derived from HeLa cells expressing this construct showed neither basal nor verapamil-stimulated ATPase activity (Figure 9). These data suggest that the linker region connecting the two halves of Pgp may be part of important structural features of the transporter needed for folding or transit to the cell surface and that insertion of a rigid structure in this region affects one or both of these processes.

Replacement of a Partial Deletion of the Linker Region of Pgp with a 17 aa Flexible Linker Peptide Restores the Ability To Confer Drug Resistance. Having determined that

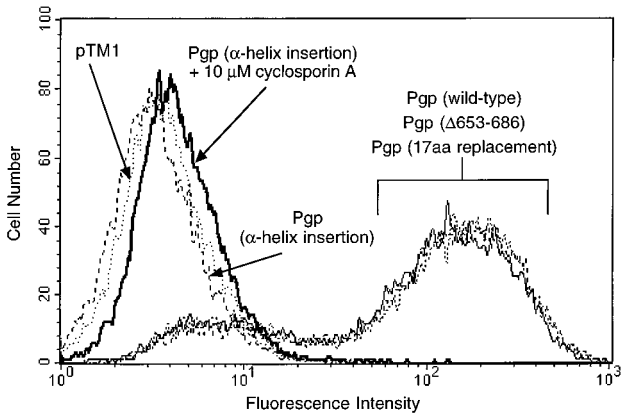

FIGURE 2: Cell surface expression of Pgp in transiently infected-transfected HeLa cells. vTF7-3-infected-transfected HeLa cells expressing wild-type Pgp (thin line), Pgp-(Δ653−686) (- - -), Pgp-(α-helix insertion) (— —), and Pgp-(17 aa replacement) (—•—) were subjected to FACS analysis after staining with MRK-16 as described in Experimental Procedures. Cells expressing Pgp-(α-helix insertion) grown in the presence of cyclosporin A (thick line) were fed with DMEM supplemented with 10% fetal bovine serum and 10 μM cyclosporin A (final concentration). Vector DNA-transfected (pTM1) cells (•••) were included as a negative control.

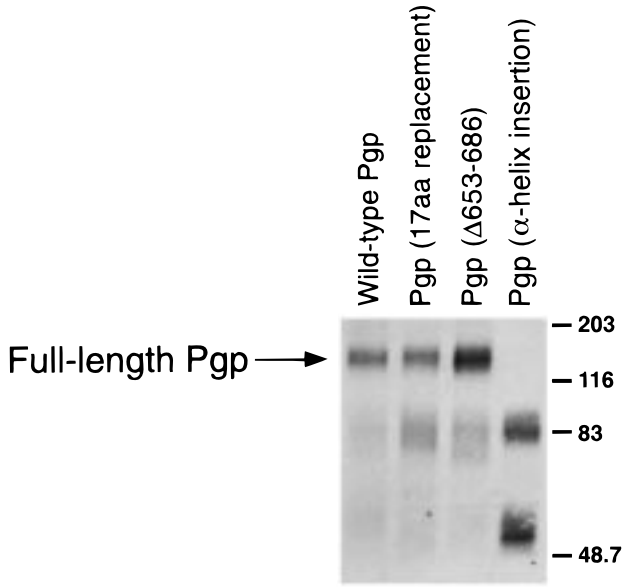

FIGURE 3: Total expression of Pgp by immunoblot analysis. HeLa cells were infected with vTF7-3 and transfected with pTM1-*MDR*1-(wild-type), pTM1-*MDR*1-(Δ653−686), pTM1-*MDR*1-(17 aa replacement), and pTM1-*MDR*1-(α-helix insertion) and harvested after 48 h. Membranes (1 μg/lane) prepared from these cells were subjected to SDS−PAGE and immunoblotting with polyclonal antibody PEPG13 (1:4000). Bands were visualized by enhanced chemiluminescence (ECL). The position of Pgp (~140 kDa) is shown by an arrow.

lengthening the linker region with a 17 aa flexible peptide had little effect on Pgp function, we deleted a portion of the linker region and subsequently replaced it with a flexible linker peptide, termed the 17 aa replacement (Figure 1B). The effects of these changes in length and composition on function, folding, and transit of the Pgp molecules to the cell surface were examined. The 17 aa replacement is comprised of mainly glycine and serine residues organized in a Gly_4Ser configuration which is predicted to be flexible (Figure 1B). This partial linker region deletion, Pgp-(Δ653−686), spans amino acids 653−686 and also includes the in vitro and in vivo serine phosphorylation sites of Pgp (*21*, *38*−*40*). NIH3T3 cells were transfected with the retroviral vectors pHa-neo (*41*), pHa*MDR*1(wild-type), pHa*MDR*1-(Δ653−686), and pHa*MDR*1-(17 aa replacement) and selected in 30 and 50 ng/mL vincristine. As shown in Table 2, transfection with the vector containing the partial deletion mutant resulted in no drug-resistant colonies, whereas the 17 aa replacement of this deletion yielded numerous vincristine-resistant colonies, albeit somewhat fewer than the wild-type construct.

Table 2: Summary of Transfections of NIH3T3 Cells with Vectors Encoding a Pgp Linker Peptide Partial Deletion and a Flexible Peptide Replacement

DNA	30 ng/mL vincristine[a]	50 ng/mL vincristine
pHa-neo	0	0
pHa*MDR*1-(wild-type)	92	69
pHa*MDR*1-(Δ653−686)	0	0
pHa*MDR*1-(17 aa replacement)	54	42

[a] Values are expressed as the number of colonies per microgram of DNA. In each experiment, duplicate 100 mm dishes were stained and the colonies counted as described in Experimental Procedures.

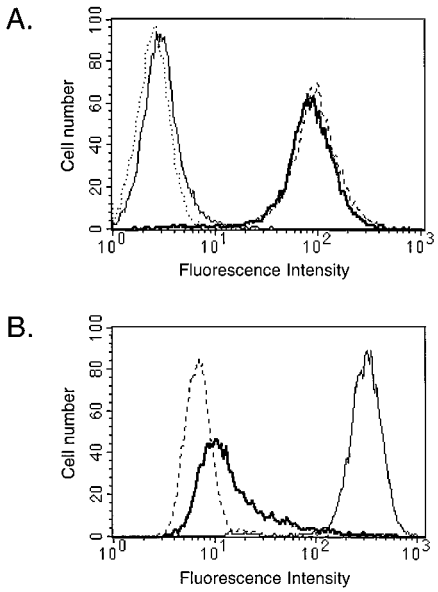

FIGURE 4: Functional expression of human Pgp in stably selected NIH3T3 cells. NIH3T3 cells were transfected with the retroviral vectors pHa-neo, pHa*MDR*1-(wild-type), pHa*MDR*1-(Δ653−686), and pHa*MDR*1-(17 aa replacement) and selected in 30 and 50 ng/mL vincristine. Drug-resistant colonies arose only upon expression of the wild-type (dashed line) and 17 aa replacement (thick line) Pgps. Cells from one 30 ng/mL 100 mm dish were pooled and analyzed for cell surface expression and function using drug-sensitive NIH3T3 cells (thin line) as a negative control. (A) Cells were stained using MRK-16 monoclonal antibody and analyzed by FACS. The nonspecific isotype control IgG2a (dotted line) was included as a negative control. (B) Rhodamine 123 accumulation was determined by FACS as described in Experimental Procedures.

The cell populations resistant to 30 ng/mL vincristine expressing wild-type Pgp and Pgp-(17 aa replacement) and drug-sensitive NIH3T3 cells were analyzed by FACS for cell surface expression and function. As shown in Figure 4A, both wild-type Pgp and the Pgp-(17 aa replacement) were expressed at comparable levels at the cell surface as determined by FACS analysis using the human Pgp-specific antibody MRK-16 that recognizes an extracellular epitope

(*16*). Because the deletion mutant was unable to confer drug resistance, it was not possible to characterize its properties in this system. Stable transfectants generated with a pHa-*MDR*1(Δ653−686)-IRES-TK-type construct (*35*) yielded HAT-selected Ltk$^-$ colonies that were also MRK-16-positive but were unable to confer cross-resistance to drugs (data not shown).

Fluorescent substrate accumulation assays were performed on the vincristine-selected NIH3T3 cells expressing wild-type Pgp and Pgp-(17 aa replacement) by FACS analysis using rhodamine 123 (Figure 4B) and calcein-AM (data not shown) as substrates. After incubation, cells expressing both constructs accumulated less of both substrates than the NIH3T3 untransfected control, as measured by a lower level of fluorescence intensity. Unlike rhodamine 123, the substrate calcein-AM itself is not fluorescent but becomes fluorescent upon cleavage by a cellular cytosolic esterase. However, this product, calcein, is no longer a Pgp substrate. This assay, therefore, measures the amount of calcein-AM that is recognized and exported by Pgp from the plasma membrane of cells (*42*). In the presence of 5 μM cyclosporin A, a known reversing agent of multidrug resistance (*2*), the Pgp-expressing cells accumulated the fluorescent compounds in a manner similar to that of the control due to inhibition of the transporter (data not shown). Taken together, these data indicate that both proteins are functional and that the observed drug resistance was due to expression of Pgp. By replacement of the 34 aa deletion with a flexible peptide sequence, transporter function was restored to greater than 80% of wild-type levels and its specificity was not altered significantly.

Partial Deletion of the Linker Region (Δ653−686) and Replacement with a 17 aa Flexible Peptide Result in Full-Length Pgp Molecules That Are Expressed at the Cell Surface. To further explore the biochemical nature of the Pgp deletion and replacement mutants and to confirm that the results were not due to the possible pleiotropic effects of the vincristine selection, these constructs were cloned into pTM1-*MDR*1 and transiently expressed in HeLa cells infected with vTF7-3 (*23*, *36*). Cell populations were subsequently assayed for total expression and for cell surface expression by immunoblot and FACS analyses. As shown in Figure 2, both the partial deletion mutant, Pgp-(Δ653−686), and the Pgp containing the 17 aa flexible replacement were expressed at the cell surface in a manner that made them indistinguishable from the wild-type protein as determined by MRK-16 staining. Total extracts from these cells were subjected to immunoblot analysis with polyclonal antibody PEPG13 and were found to be expressed at levels comparable to wild-type Pgp (Figure 3). A 140 kDa band was expected because Pgp expressed using the vaccinia virus transient expression system appears to be underglycosylated (*23*). However, it has been established that complete glycosylation is not essential for the proper functioning of Pgp (*43*−*45*). When the gel was allowed to run for an extended period of time, Pgp-(Δ653−686) demonstrated an increased mobility due to the deletion of the 34 aa peptide from the linker region and/or lack of the phosphorylation sites (data not shown).

Partial Deletion of the Linker Region Abrogates Function That Can Be Restored by the Addition of the 17 aa Flexible Replacement Linker Peptide. HOS cells were transiently

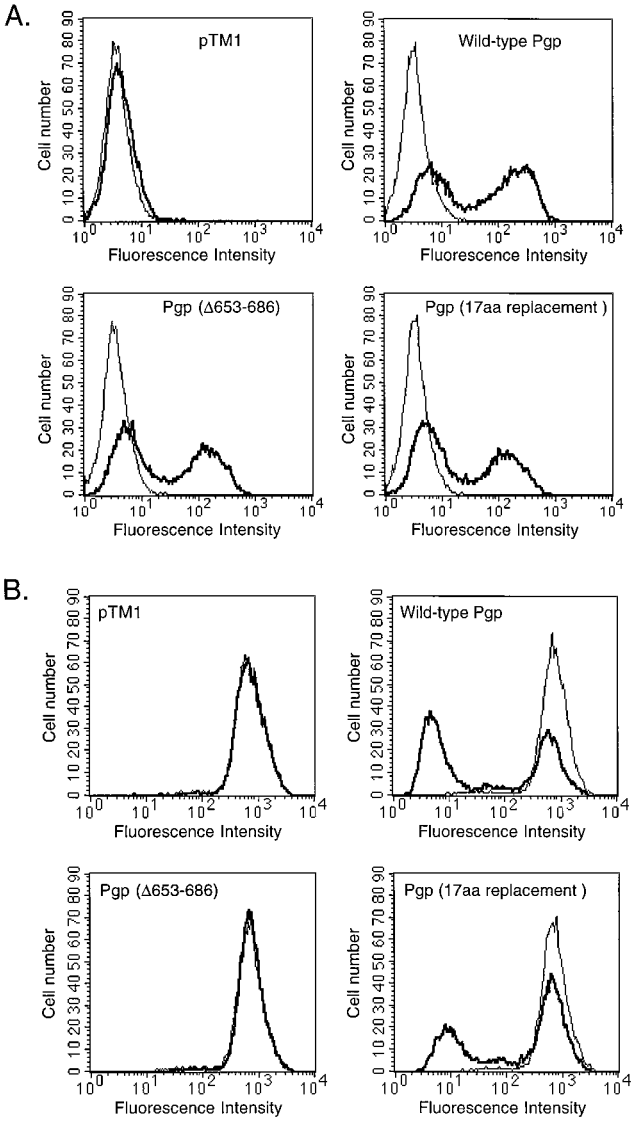

FIGURE 5: Expression and functional analysis of Pgp in transiently infected-transfected HOS cells. HOS cells were infected with vTF7-3 and transfected with pTM1-*MDR*1-(wild-type), pTM1-*MDR*1-(Δ653−686), and pTM1-*MDR*1-(17 aa replacement) for 24 h. (A) Cells were subjected to FACS analysis after MRK-16 staining (thick line). Samples were assayed in parallel with the IgG2a isotype control antibody (thin line). (B) Rhodamine 123 accumulation was determined in these cells in the presence (thin line) and absence (thick line) of 7.5 μM cyclosporin A. In all experiments, vTF7-3-infected cells transfected with pTM1 vector DNA were included as controls.

infected with vTF7-3 and transfected with pTM1-*MDR*1-(wild-type), the deletion mutant, pTM1-*MDR*1-(Δ653−686), the 17 aa flexible replacement mutant, pTM1-*MDR*1-(17 aa replacement), and pTM1 as a negative control. HOS cells were chosen for these studies because they are more amenable to fluorescent drug accumulation studies than HeLa cells due to reduced background (*23*). After approximately 24 h, cells were analyzed for cell surface expression by MRK-16 staining (Figure 5A). The mutant Pgps are expressed at slightly reduced levels compared to wild-type Pgp in these cells. These proteins were subsequently examined in fluorescent drug accumulation experiments using rhodamine 123 (Figure 5B). As was observed for the stable NIH3T3 transfectants (Figure 4B), wild-type Pgp and Pgp containing the 17 aa flexible replacement linker were

functional as demonstrated by the lowered fluorescence intensity compared to the pTM1 control cells. In the presence of 5 μM cyclosporin A, Pgp function was inhibited and the cells accumulated the fluorescent compounds in a manner similar to that of the pTM1 control. Strikingly, the Pgp-(Δ653−686) deletion mutant was completely nonfunctional as demonstrated by an accumulation pattern that was indistinguishable from that of the pTM1 control cells, both in the presence and in the absence of 5 μM cyclosporin A (Figure 5B). Similar data were obtained for other fluorescent substrates, including calcein-AM, bodipy-FL-verapamil, and daunorubicin (data not shown).

[^{125}I]IAAP and [α-^{32}P]-8-Azido-ATP Binding Are Minimally Affected in the Partial Linker Region Deletion Mutant. The drug and nucleotide binding properties of the Pgp deletion mutant and the 17 aa flexible replacement Pgp mutant were examined by photaffinity labeling studies using [^{125}I]IAAP, a substrate analogue, and [α-^{32}P]-8-azido-ATP, a nucleotide analogue. HeLa cells were transiently infected with vTF7-3 and transfected with pTM1-*MDR*1-(wild-type), the deletion mutant, pTM1-*MDR*1-(Δ653−686), the 17 aa flexible replacement mutant, pTM1-*MDR*1-(17 aa replacement peptide), and pTM1 as a negative control and incubated for approximately 24 h. Whole cells were labeled with [^{125}I]-IAAP in the presence and absence of 10 μM cyclosporin A as a reversing agent to determine the specificity of labeling. Efficient photoaffinity labeling of the deletion mutant was observed and appeared to be comparable to that of the wild-type protein. The labeling was specific as demonstrated by the elimination of labeling in the presence of cyclosporin A (Figure 6). The dark band in the second through fourth lanes at approximately 80 kDa most likely represents the amino-terminal fragment of the full-length molecule where labeling with [^{125}I]IAAP was inhibited by cyclosporin A. Additionally, labeling of the partial linker region deletion mutant was stimulated by the addition of 100 μM *cis*-(*Z*)-flupentixol, a compound that is known to stimulate [^{125}I]IAAP labeling to the C-terminal half of wild-type Pgp (data not shown) (*46*, *47*). The Pgp-(17 aa replacement) mutant also resulted in a protein that was labeled by [^{125}I]IAAP in a manner indistinguishable from that of the wild-type protein. These data suggest that the substrate binding properties of the deletion mutant appear to be minimally affected by removal of the 34 amino acids.

Crude membrane preparations of HeLa cells expressing wild-type Pgp, the Pgp-(Δ653−686) deletion mutant, and Pgp containing the 17 aa peptide replacement were photoaffinity labeled with [α-^{32}P]-8-azido-ATP, immunoprecipitated with PEPG13, and subjected to SDS−PAGE and autoradiography (Figure 7). Membranes derived from HeLa cells infected with vTF7-3 alone were used as a control. As expected, no band was observed in the vTF7-3 control lane. The data from the other lanes suggest that there is little to no impairment of the ability of these constructs to be photoaffinity labeled by [α-^{32}P]-8-azido-ATP compared to that of the wild-type molecule. Addition of 500 μM EDTA to incubations prepared in magnesium-free buffer completely eliminated photoaffinity labeling, indicating that the labeling was magnesium-dependent (data not shown).

Basal and Verapamil-Stimulated ATPase Activity Is Absent in the Linker Region Deletion Mutant and Regained in the Pgp Mutant Containing the 17 aa Flexible Replacement Peptide. Orthovanadate is a phosphate analogue that stabilizes the catalytic transition state of Pgp (Pgp·Mg^{2+}ADP·Vi), mimicking the physiological state in which Mg^{2+}ADP and phosphate are bound and subsequently released (*48*). This phenomenon serves as the basis for a sensitive assay for determining the ability of a Pgp molecule to hydrolyze ATP (*48*). When 300 μM vanadate was included in the assay under hydrolytic conditions in the absence of substrate, a significant increase in the amount of label was observed for the wild-type and the 17 aa peptide replacement (Figure 8). However, no detectable increase was observed for the deletion mutant. These results suggest that the ability to hydrolyze ATP was severely impaired in the deletion mutant compared to the wild type and restored by addition of the flexible 17 aa peptide replacement.

The verapamil-stimulated ATPase activity of the various Pgp constructs synthesized in HeLa cells with the vaccinia T7 system was measured as the vanadate-sensitive release of inorganic phosphate from Mg^{2+}ATP (Figure 9). Membrane preparations from vTF7-3-infected cells demonstrated an ATPase activity of ∼7−8 nmol min^{-1} (mg of membrane protein)$^{-1}$ that did not increase when assayed in the presence of 25 μM verapamil. The basal membrane-associated ATPase activity increased to 12−18 nmol min^{-1} (mg of membrane protein)$^{-1}$ upon expression of wild-type Pgp. This activity was stimulated approximately 2−2.8-fold in the presence of 25 μM verapamil. The deletion Pgp mutant (Δ653−686) demonstrated neither basal nor verapamil-

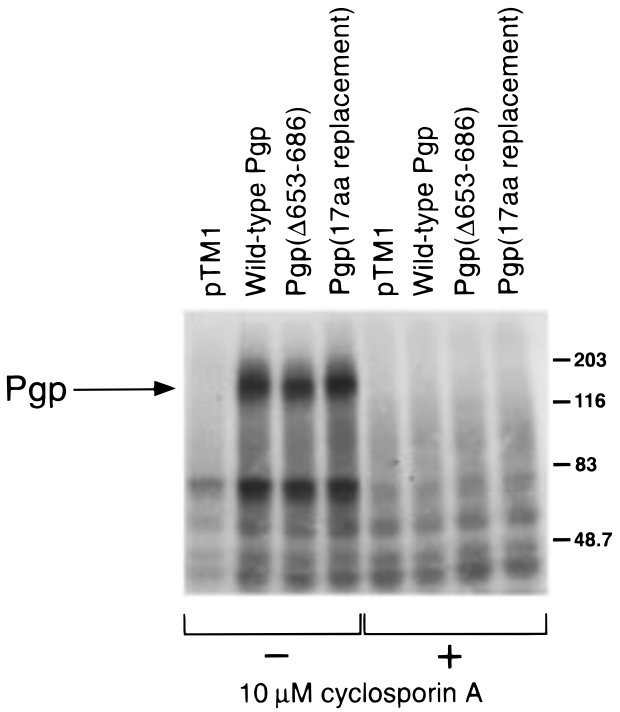

FIGURE 6: Photoaffinity labeling of Pgp in transiently infected-transfected HeLa cells. Intact HeLa cells infected with vTF7-3 and transfected with pTM1-*MDR*1-(wild-type), pTM1-*MDR*1-(Δ653−686), and pTM1-*MDR*1-(17 aa replacement) for 24 h were photoaffinity labeled with [^{125}I]IAAP as described in Experimental Procedures. After labeling, total cell lysates were subjected to SDS−PAGE and autoradiography. Where indicated, 10 μM cyclosporin A was added as a competitor to determine the specificity of labeling. vTF7-3-infected cells transfected with pTM1 vector DNA were included as a negative control. The position of Pgp (∼140 kDa) is shown by an arrow.

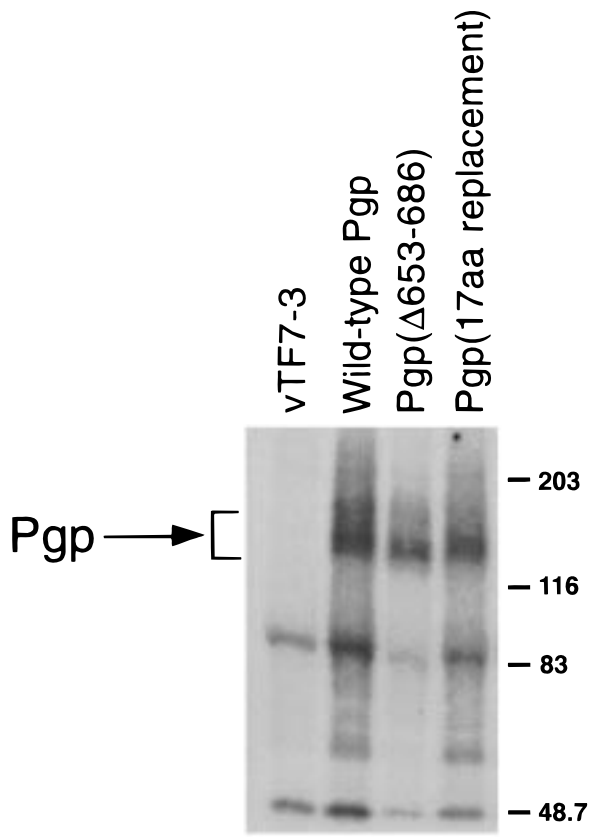

FIGURE 7: [α-^{32}P]-8-Azidoadenosine 5′-triphosphate ([α-^{32}P]-8-azido-ATP) labeling of Pgp in membrane preparations of transiently infected-transfected HeLa cells. Membrane preparations (50 μg) from HeLa cells infected with vTF7-3 and transfected with pTM1-*MDR*1-(wild-type), pTM1-*MDR*1-(Δ653−686), and pTM1-*MDR*1-(17 aa replacement) were photoaffinity labeled with [α-^{32}P]-8-azido-ATP and subjected to immunoprecipitation with polyclonal antibody PEPG13 as described in Experimental Procedures. Eluants were analyzed by SDS−PAGE and autoradiography. Membrane preparations from HeLa cells infected with vTF7-3 alone were used as the negative control. The position of Pgp (∼140 kDa) is shown by an arrow.

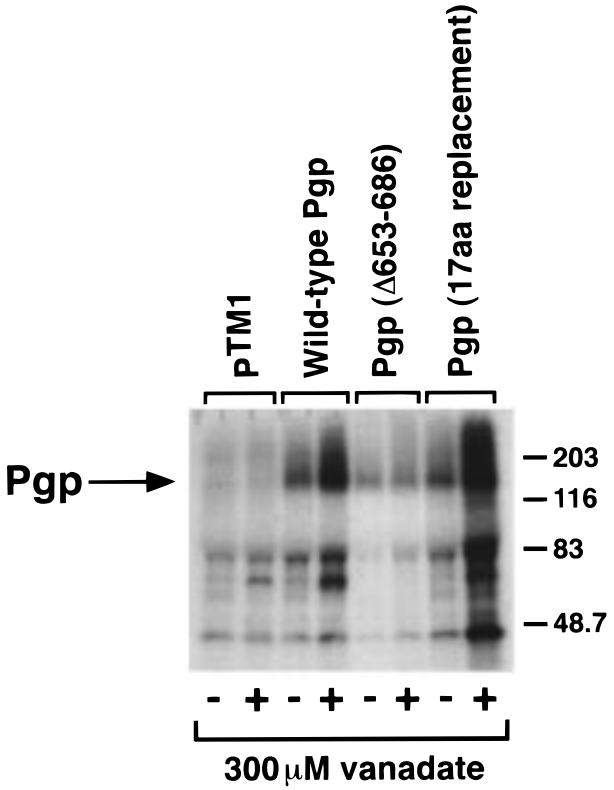

FIGURE 8: [α-^{32}P]-8-Azidoadenosine 5′-triphosphate ([α-^{32}P]-8-azido-ATP) labeling and vanadate trapping of human Pgp in membranes of transiently infected-transfected HeLa cells. Membrane preparations (50 μg) from HeLa cells infected with vTF7-3 and transfected with pTM1 (negative control), pTM1-*MDR*1-(wild-type), pTM1-*MDR*1-(Δ653−686), and pTM1-*MDR*1-(17 aa replacement) were photoaffinity labeled with [α-^{32}P]-8-azido-ATP in the presence and absence of 300 μM sodium orthovanadate as described in Experimental Procedures and subjected to immunoprecipitation with polyclonal antibody PEPG12. In this experiment, 10 mM $CoCl_2$ was substituted for $MgCl_2$ to increase the efficiency of the reaction (*48*, *50*). Eluants were analyzed by SDS−PAGE and autoradiography. The position of Pgp (∼140 kDa) is shown by an arrow.

stimulated ATPase activity above the vTF7-3 control. Importantly, upon replacement of the 17 aa flexible linker peptide into this deletion mutant, both the basal and verapamil-stimulated ATPase activities were restored to approximately 80−90% of wild-type Pgp levels, suggesting that the two halves of Pgp must be separated by a flexible linker for normal basal and substrate-stimulated ATPase activity to facilitate the functional interaction of these domains.

The Linker Region Deletion Mutant Has a Conformation Altered from Those of the Wild-Type and the Pgp-(17 aa Replacement) Proteins on the Basis of Interaction with the Conformation-Sensitive and ATP Hydrolysis-Dependent Monoclonal Antibody UIC2. The reactivity of the various Pgp constructs expressed in HeLa cells with the vaccinia T7 system with the human Pgp-specific monoclonal antibody UIC2 was measured in the presence and absence of 5 μM cyclosporin A (*49*). As shown in Figure 10B, the wild-type protein demonstrates a significant increase in UIC2 reactivity when incubated in the presence of cyclosporin A. In marked contrast, the partial deletion mutant, Pgp-(Δ653−686), shows no difference in reactivity and is equivalent to the cyclosporin A-treated cells expressing wild-type Pgp (Figure 10C). The Pgp containing the 17 aa flexible replacement demonstrated an intermediate effect (Figure 10D). Cyclosporin A incubation in cells not expressing Pgp had no measurable effect (Figure 10A). All cells treated with cyclosporin A, regardless of which Pgp was expressed, were indistinguishable by FACS analysis. Experiments with MRK-16 showed that all constructs were similarly expressed on the surface and that cyclosporin A treatment had no effect (Figure 2 and data not shown). The data presented here suggest that inactive Pgp molecules exist in a different conformation in the cell. It has also been demonstrated that upon treatment of cells with azide and deoxyglucose or other ATP-depleting agents, the Pgp population shifts to a position consistent with the inactive state (*49*; data not shown). Importantly, we have also demonstrated that upon the addition of glucose (i.e., energy) to these depleted cells, the population shifts back to the active state (data not shown). These data are consistent with a model in which the wild-type Pgp molecule transiently cycles through the inactive conformation during the transport process.

Although it has been suggested that this inactive conformation can be attributed to the inability of the molecule to bind ATP (*49*), these and additional results (C. A. Hrycyna

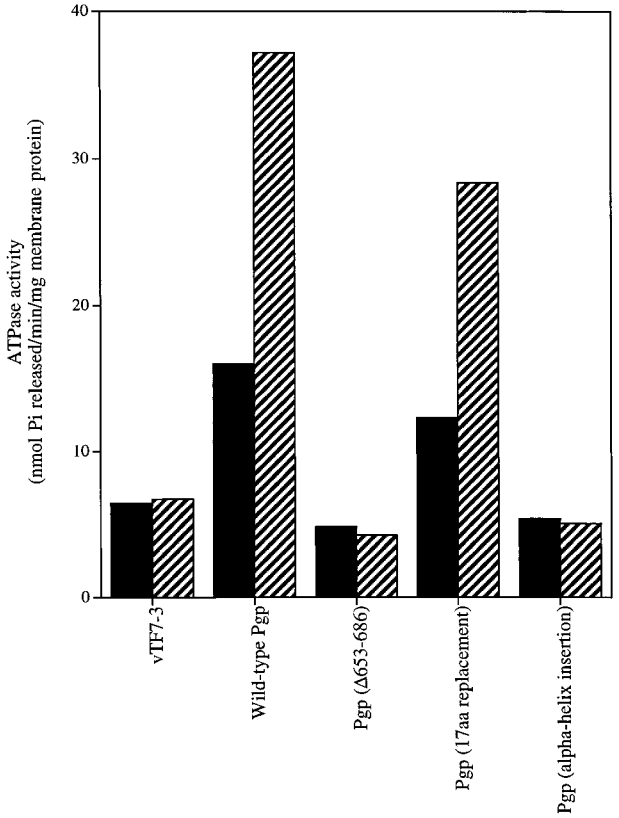

FIGURE 9: Basal and verapamil-stimulated ATPase activities of Pgp in membranes of transiently infected-transfected HeLa cells. Membrane preparations from HeLa cells infected with vTF7-3 and transfected with pTM1-*MDR*1-(wild-type), pTM1-*MDR*1-(Δ653−686), pTM1-*MDR*1-(17 aa replacement), and pTM1-*MDR*1-(α-helix insertion). The vanadate-sensitive activities shown represent the difference between the ATPase activities measured in the presence and absence of 300 μM vanadate. Basal activity (dark bars) was measured without the addition of verapamil. Stimulated activity (striped bars) was determined in the presence of 25 μM verapamil. Membrane preparations from HeLa cells infected with vTF7-3 alone were used as the negative control. These experiments were repeated a minimum of three times with different preparations of membranes with the same relative results.

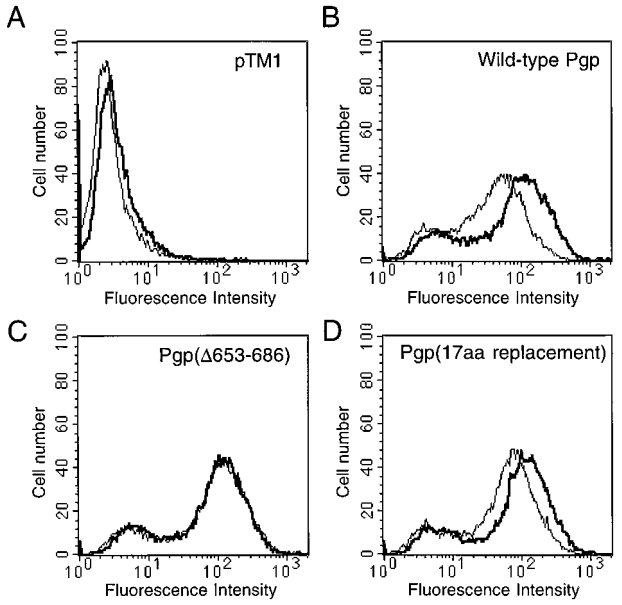

FIGURE 10: UIC2 reactivity shift induced by incubation with cyclosporin A. vTF7-3-infected-transfected HeLa cells expressing wild-type Pgp (B), Pgp-(Δ653−686) (C), and Pgp-(17 aa replacement) (D) were subjected to FACS analysis after staining with UIC2 in the presence (thick line) and absence (thin line) of 5 μM cyclosporin A as described in Experimental Procedures. Vector DNA-transfected (pTM1) cells (A) were included as a negative control.

and S. V. Ambudkar, unpublished results) strongly suggest that these conformational changes are measures of the ability of the Pgp molecule to hydrolyze ATP. All of the Pgp molecules examined here are capable of binding ATP (Figure 7), but only wild-type Pgp and the Pgp containing the 17 aa peptide replacement are capable of hydrolyzing ATP (Figures 8 and 9) and demonstrate an increase in reactivity when incubated with cyclosporin A (Figure 10). Additionally, these conformational data correlate with the ATPase data since the Pgp containing the 17 aa peptide replacement has less measurable ATPase activity and also demonstrates a less dramatic shift in UIC2 reactivity in the presence of cyclosporin A.

DISCUSSION

The human *MDR*1 cDNA encodes a 1280 aa protein with two homologous halves. Each half contains six hydrophobic transmembrane regions implicated in binding of substrates and inhibitors on the basis of photoaffinity labeling studies and the behavior of mutant transporters and a highly conserved ATP binding/utilization domain (*2*). On the basis of this primary structure of Pgp and its internal homology, two basic models may be proposed for its functional organization: (1) a "double-barreled model" in which the amino- and carboxyl-terminal halves are hypothesized to be connected but to operate independently with each half containing a distinct site or sites for drug binding and transport and (2) a "single-barreled model" in which the amino- and carboxyl-terminal halves interact to form a single functional unit with multiple substrate binding sites (*46*) and alternating, nonconcurrent catalysis at the two ATP sites (*50*, *60*). At present, most of the data from mutational analysis, photoaffinity labeling, and ATP utilization studies favor the single-barreled model (*1*, *2*). The results reported in this paper showing that changes in the flexible connecting region between the amino- and carboxyl-terminal halves of Pgp result in a loss of ability of substrates to stimulate ATPase activity, despite intact substrate binding and ATP sites, are also consistent with the single-barreled model, but do not prove it.

The experiments presented here were designed to assess the importance of the length, structure, and composition of the nonconserved 75 aa segment that connects the two halves of Pgp by deletion and insertion mutagenesis. In the previously discussed single-barreled model for the tertiary structure of Pgp, a small rigid insertion would be predicted to disturb the interface between the amino- and carboxyl-terminal halves, thereby disabling transport; whereas in the double-barreled model where each half would act autonomously, transport function may not be affected. In either of these two scenarios, lengthening of the linker region with a flexible peptide would not necessarily be predicted to elicit deleterious effects on function. A modified Pgp with a flexible amino acid insertion peptide in the linker region was found to confer drug resistance when transfected into NIH3T3 cells. This result argues that extending the length

of the connecting region by 17 amino acids does not have serious detrimental consequences on Pgp function. In fact, the R domain of CFTR, homologous to the linker region of Pgp, is considerably longer, suggesting that even longer stretches might be tolerated in this region of Pgp. Insertion of a sequence of similar length but possessing a more defined α-helical structure resulted in a protein that was not expressed on the cell surface, did not possess any ATPase activity in vitro, and was rapidly degraded. These results suggest that the α-helical peptide insertion into the linker region prevented proper folding of the other domains of P-glycoprotein or that the inserted peptide may be interacting with another part of the molecule causing an alteration in structure.

The deletion mutant described in this paper is the first example of a mutant outside of the known substrate and ATP binding sites in which the levels of both substrate and ATP binding are similar to those of the wild-type molecule, but basal and drug-stimulated ATP hydrolysis are abrogated. Moreover, the linker region deletion mutant also provides an example of an inactive Pgp molecule that comes to the cell surface in a manner similar to that of the wild-type protein. It is expected that mutants of this type will serve as standards for both two- and three-dimensional structural studies of Pgp since the mutant and wild-type both fold reasonably well and appear at the cell surface, but only one allows substrate to stimulate ATPase activity and subsequent drug transport.

We have also determined differential conformational states of Pgp that are dependent upon ATP hydrolysis and not necessarily upon ATP binding as previously suggested (*49*). Our mutants described here have similar abilities to bind ATP, but only the hydrolysis-competent molecules are capable of exhibiting an increased reactivity with UIC2 in the presence of substrates. As demonstrated here, mutants that are incapable of hydrolyzing ATP are recognized similarly by UIC2 as those functional molecules that have been incubated in the presence of drug. These two conformational states most likely represent transport-competent and transport-incompetent forms of Pgp (*49*). Our data suggest that the ability of a Pgp molecule to hydrolyze ATP, and thus transport substrates, can be monitored by the substrate-dependent UIC2 reactivity and demonstrate that in the absence of substrate, ATP hydrolysis-competent Pgp molecules are recognized less well by UIC2 than inactive molecules.

It is important to note that the linker region of Pgp and, in fact, the linker regions of many members of the ABC superfamily, is comprised of multiple charged amino acid residues (*51*). These residues do not appear to be essential for localization to the plasma membrane or for binding of drugs or ATP since a deletion of 34 amino acids from the central core of the linker region that contained 13 charged residues resulted in a transporter that was fully able to carry out these functions. However, this deletion was incapable of conferring drug resistance or transporting fluorescent substrates and was devoid of any basal or drug-stimulated ATPase activity. The fact that the transport and ATPase activities of the protein were abrogated suggests that the two halves of Pgp must be separated and that the cooperative interaction or spatial orientation of the two halves may have been disrupted. These interactions between the two halves could involve the two ATP sites, the ATP sites and the drug binding sites, or both. Upon reintroduction of an uncharged flexible peptide comprised mainly of glycine and serine residues which nearly restored the original length of the linker region, function was reconstituted to near wild-type levels as determined in both transient and stable cell lines in both in vitro and in vivo assays. These results lend strong evidence to support the single-barreled model of Pgp functional organization, but are not consistent with a critical function for the charged residues.

For another member of the ABC family, the yeast **a**-factor transporter, STE6, the highly charged nature of the linker region appears to serve a different role. It has been determined that an acidic stretch of amino acids (609−661), containing the motif DAKTI, may be important in the rapid ubiquitin-mediated turnover of the protein (*52*). Interestingly, deletion of this region resulted in a fully functional STE6 molecule that had a half-life that was 5 times greater than that of the wild-type protein. This DAKTI motif is not present in human Pgp, and in fact, human Pgp, which has a half-life of >48 h, has not been found to be ubiquitinated (*53*).

Previous studies have indicated that Pgp can exist as monomers, dimers, or higher-order oligomers in native membranes and that the dynamics of oligomer formation may be important in the mechanism of action of Pgp (*54*−*57*). The linker region has been implicated in the assembly of higher-order oligomers of Pgp. By expressing amino acids 621−688 from the linker region of murine *mdr*1b Pgp as a glutathione *S*-transferase fusion protein, Juvvadi et al. (*58*) demonstrated that this highly charged peptide exists as a noncovalent dimer in solution, presumably due to ionic interactions. Our studies presented here in which replacing amino acids 653−686 with an uncharged flexible peptide resulted in a highly functional transporter in vivo suggest that this phenomenon, if occurring in vivo, is not critical for Pgp function. In fact, by differential epitope tagging, it was determined that the minimal functional unit of Pgp appears to be a monomer (*59*).

Similar to the highly charged R domain of CFTR, the linker region of human Pgp as well as other Pgps from different species also contains multiple consensus sequences for phosphorylation by protein kinases such as protein kinase A and C that require basic amino acid residues near the phosphoacceptor group (*1*). It has been hypothesized that phosphorylation of these residues may regulate the activity of Pgp (*21*, *38*, *40*). However, recent experiments in which the major phosphorylation sites (serines 661, 667, 671, 675, and 683) (Figure 1A) were changed to alanine residues or to aspartate residues resulted in Pgp molecules that were fully able to confer resistance to cytotoxic drugs, suggesting that phosphorylation and dephosphorylation may not be essential for the overall activity of the transporter (*21*). In this study, a Pgp molecule that replaced the peptide segment containing these major serine phosphorylation sites with a 17 aa flexible peptide, not containing any phosphorylation consensus sequences, was constructed. This protein was functional both in vitro and in vivo, albeit with slightly reduced activity compared to the wild type. Taken together with the mutational study of the phosphorylation sites described above, this slight reduction in activity was presumably due to nonideal interaction of the two halves of Pgp, most likely the two ATP sites, as the deletion mutant is devoid of even

basal ATPase activity as determined by vanadate trapping experiments.

Our data strongly suggest that the major role of the flexible linker region of human Pgp is to permit proper intramolecular interactions between the two ATP sites. However, we cannot ignore the fact that through evolution this region has remained highly charged with conservation of multiple sites for phosphorylation. Although this structure of the linker region may be fortuitous, we cannot rule out other as yet to be determined functions for this region, including the possibility that it may play a more subtle role in protein targeting, or that it may regulate function of Pgp via interactions with other cellular factors.

REFERENCES

1. Gottesman, M. M., Hrycyna, C. A., Schoenlein, P. V., Germann, U. A., and Pastan, I. (1995) *Annu. Rev. Genet. 29*, 607−649.
2. Gottesman, M. M., and Pastan, I. (1993) *Annu. Rev. Biochem. 62*, 385−427.
3. Chen, C.-j., Chin, J. E., Ueda, K., Clark, D. P., Pastan, I., Gottesman, M. M., and Roninson, I. B. (1986) *Cell 47*, 381−389.
4. Horio, M., Gottesman, M. M., and Pastan, I. (1988) *Proc. Natl. Acad. Sci. U.S.A. 85*, 3580−3584.
5. Gottesman, M. M., and Pastan, I. (1988) *J. Biol. Chem. 263*, 12163−12166.
6. Muller, M., Bakos, E., Welker, E., Varadi, A., Germann, U. A., Gottesman, M. M., Morse, B. S., Roninson, I. B., and Sarkadi, B. (1996) *J. Biol. Chem. 271*, 1877−1883.
7. Currier, S. J., Ueda, K., Willingham, M. C., Pastan, I., and Gottesman, M. M. (1989) *J. Biol. Chem. 264*, 14376−14381.
8. Loo, T. W., and Clarke, D. M. (1994) *J. Biol. Chem. 269*, 7750−7755.
9. Germann, U. A. (1996) *Eur. J. Cancer 32A*, 927−944.
10. Schinkel, A. H., and Borst, P. (1991) *Semin. Cancer Biol. 2*, 213−226.
11. Buschman, E., and Gros, P. (1991) *Mol. Cell. Biol. 11*, 595−603.
12. Chen, C.-j., Clark, D., Ueda, K., Pastan, I., Gottesman, M. M., and Roninson, I. B. (1990) *J. Biol. Chem. 265*, 506−514.
13. Riordan, J. R., Rommens, J. M., Kerem, B.-s., Alon, N., Rozmahel, R., Grzelczak, A., Aielenski, J., Lok, S., Plavsic, N., Chou, J.-l., Drumm, M. L., Iannuzzi, M. C., Collins, F. S., and Tsui, L.-c. (1989) *Science 245*, 1066−1073.
14. Elroy-Stein, O., and Moss, B. (1991) in *Current Protocols in Molecular Biology* (Ausubel, F. M., Brent, R., Kinston, R. E., Moore, D. D., Smith, J. A., Seidman, J. C., and Struhl, K., Eds.) pp 16.19.1−16.19.9, John Wiley and Sons, New York.
15. Earl, P. E., Cooper, N., and Moss, B. (1991) in *Current Protocols in Molecular Biology* (Ausubel, F. M., Brent, R., Kinston, R. E., Moore, D. D., Smith, J. A., Seidman, J. C., and Struhl, K., Eds.) pp 16.16.1−16.16.7, John Wiley and Sons, New York.
16. Hamada, H., and Tsuruo, T. (1986) *Proc. Natl. Acad. Sci. U.S.A. 83*, 7785−7789.
17. Bruggemann, E. P., Chaudhary, V., Gottesman, M. M., and Pastan, I. (1991) *BioTechniques 10*, 202−209.
18. Sanger, F., Nicklen, S., and Coulsen, A. R. (1977) *Proc. Natl. Acad. Sci. U.S.A. 74*, 5463−5467.
19. Pastan, I., Gottesman, M. M., Ueda, K., Lovelace, E., Rutherford, A. V., and Willingham, M. C. (1988) *Proc. Natl. Acad. Sci. U.S.A. 85*, 4486−4490.
20. Kane, S. E., and Gottesman, M. M. (1993) in *Methods Enzymol. 217*, 34−47.
21. Germann, U. A., Chambers, T. C., Ambudkar, S. V., Licht, T., Cardarelli, C. O., Pastan, I., and Gottesman, M. M. (1996) *J. Biol. Chem. 271*, 1708−1716.
22. Choi, K., Chen, C.-J., Kriegler, M., and Roninson, I. B. (1989) *Cell 53*, 519−529.
23. Ramachandra, M., Ambudkar, S. V., Gottesman, M. M., Pastan, I., and Hrycyna, C. A. (1996) *Mol. Biol. Cell 7*, 1485−1498.
24. Sambrook, J., Fritsch, E. F., and Maniatis, T. (1989) *Molecular cloning, a laboratory manual*, Cold Spring Harbor Laboratory Press, Plainview, NY.
25. Loo, T. W., and Clarke, D. M. (1995) *J. Biol. Chem. 270*, 21449−21452.
26. Kioka, N., Tsubota, J., Kakehi, Y., Komano, T., Gottesman, M. M., Pastan, I., and Ueda, K. (1989) *Biochem. Biophys. Res. Commun. 162*, 224−231.
27. Shen, D.-w., Fojo, A. T., Roninson, I. B., Soffir, R., Pastan, I., and Gottesman, M. M. (1986) *Mol. Cell. Biol. 6*, 4039−4045.
28. Bailey, J. L. (1967) *Techniques in Protein Chemistry*, pp 340−341, Elsevier Publishing Co., New York.
29. Laemmli, U. K. (1970) *Nature 227*, 680−685.
30. Bruggemann, E. P., Germann, U. A., Gottesman, M. M., and Pastan, I. (1989) *J. Biol. Chem. 264*, 15483−15488.
31. Sarkadi, B., Price, E. M., Boucher, R. C., Germann, U. A., and Scarborough, G. A. (1992) *J. Biol. Chem. 267*, 4854−4858.
32. Chaudhary, V. K., Queen, C., Junghans, R. P., Waldmann, T. A., FitzGerald, D. J., and Pastan, I. (1989) *Nature 339*, 394−397.
33. Marqusee, S., Robbins, V. H., and Baldwin, R. L. (1989) *Proc. Natl. Acad. Sci. U.S.A. 86*, 5286−5290.
34. Marqusee, S., and Baldwin, R. L. (1987) *Proc. Natl. Acad. Sci. U.S.A. 84*, 8898−8902.
35. Sugimoto, Y., Aksentijevich, I., Gottesman, M. M., and Pastan, I. (1994) *Bio/Technology 12*, 694−698.
36. Hrycyna, C. A., Zhang, S., Ramachandra, M., Ni, B., Pastan, I., and Gottesman, M. M. (1996) in *Multidrug Resistance in Cancer Cells: Cellular, Biochemical, Molecular and Biological Aspects* (Gupta, S., and Tsuruo, T., Eds.) pp 29−37, John Wiley and Sons, New York.
37. Loo, T. W., and Clarke, D. M. (1997) *J. Biol. Chem. 272*, 709−712.
38. Orr, G. A., Han, E. K.-H., Browne, P. C., Nieves, E., O'Connor, B. M., Yang, C. P., and Horwitz, S. B. (1993) *J. Biol. Chem. 268*, 25054−25062.
39. Chambers, T. C., Zheng, B., and Kuo, J. F. (1992) *Mol. Pharmacol. 41*, 1008−1015.
40. Chambers, T. C., Pohl, J., Raynor, R. L., and Kuo, J. F. (1993) *J. Biol. Chem. 268*, 4592−4595.
41. Markowitz, D., Goff, S., and Bank, A. (1988) *J. Virol. 62*, 1120−1124.
42. Hollo, Z., Homolya, L., Davis, C. W., and Sarkadi, B. (1994) *Biochim. Biophys. Acta 1191*, 384−388.
43. Beck, W. T., and Cirtain, M. (1982) *Cancer Res. 42*, 184−189.
44. Germann, U. A., Willingham, M. C., Pastan, I., and Gottesman, M. M. (1990) *Biochemistry 29*, 2295−2303.
45. Schinkel, A. H., Kemp, S., Dolle, M., Rudenko, G., and Wagenaar, E. (1993) *J. Biol. Chem. 268*, 7474−7481.
46. Dey, S., Ramachandra, M., Pastan, I., Gottesman, M. M., and Ambudkar, S. V. (1997) *Proc. Natl. Acad. Sci. U.S.A. 94*, 10594−10599.
47. Safa, A. R., Agresti, M., Bryk, D., and Tamai, I. (1994) *Biochemistry 33*, 256−265.
48. Urbatsch, I. L., Sankaran, B., Weber, J., and Senior, A. E. (1995) *J. Biol. Chem. 270*, 19383−19390.
49. Mechetner, E. B., Schott, B., Morse, B. S., Stein, W. D., Druley, T., Davis, K. A., Tsuruo, T., and Roninson, I. B. (1997) *Proc. Natl. Acad. Sci. U.S.A. 94*, 12908−12913.

50. Urbatsch, I. L., Sankaran, B., Bhagat, S., and Senior, A. E. (1995) *J. Biol. Chem. 270*, 26956−26961.
51. Germann, U. A. (1993) *Cytotechnology 12*, 33−62.
52. Kolling, R., and Losko, S. (1997) *EMBO J. 16*, 2251−2261.
53. Jensen, T. J., Loo, M. A., Pind, S., Williams, D. B., Goldberg, A. L., and Riordan, J. R. (1995) *Cell 83*, 129−135.
54. Georges, E., Tsuruo, T., and Ling, V. (1993) *J. Biol. Chem. 268*, 1792−1798.
55. Boscoboinik, D., Debanne, M. T., Stafford, A. R., Jung, C. Y., Gupta, R. S., and Epand, R. M. (1990) *Biochim. Biophys. Acta 1027*, 225−228.
56. Poruchynsky, M. S., and Ling, V. (1994) *Biochemistry 33*, 4163−4174.
57. Naito, M., and Tsuruo, T. (1992) *Biochem. Biophys. Res. Commun. 185*, 284−290.
58. Juvvadi, S. R., Glavy, J. S., Horwitz, S. B., and Orr, G. A. (1997) *Biochem. Biophys. Res. Commun. 230*, 442−447.
59. Loo, T. W., and Clarke, D. M. (1996) *J. Biol. Chem. 271*, 27488−27492.
60. Hrycyna, C. A., Ramachandra, M. R., Ambudkar, S. V., Ko, Y. H., Pedersen, P. L., Pastan, I., and Gottesman, M. M. (1998) *J. Biol. Chem. 273*, 16631−16634.

BI9808823